Sterically stabilized colloidal dispersions: beyond hard spheres

1999 J. Phys.: Condens. Matter 11 10119

(http://iopscience.iop.org/0953-8984/11/50/306)

J. Phys.: Condens. Matter **11** (1999) 10119–10131. Printed in the UK PII: S0953-8984(99)06456-5

Sterically stabilized colloidal dispersions: beyond hard spheres

Moises Silbert†, Enrique Canessa‡, Malcolm J Grimson§ and Osvaldo H Scalise‖

† School of Chemical Sciences, University of East Anglia, Norwich NR4 7TJ, UK
‡ The Abdus Salam International Centre for Theoretical Physics (ICTP), PO Box 586, 34100 Trieste, Italy
§ Department of Physics, University of Auckland, Private Bag 92019, Auckland, New Zealand
‖ Instituto de Física de Líquidos y Sistemas Biológicos (IFLYSIB), CC 565, (1900) La Plata, Argentina

Received 30 July 1999, in final form 14 October 1999

Abstract. Sterically stabilized colloidal dispersions, such as PMMA, have long been regarded as archetypal realizations of hard spheres and hard-sphere mixtures. Indeed, this is precisely what is found in studies of these systems as a function of the volume fraction, at constant temperature. However, a much richer behaviour—which goes beyond what is expected from just hard spheres—is found as a function of both volume fraction and temperature T. For instance, sterically stabilized colloids are known to exhibit both upper (high-T) and lower (low-T) two-phase behaviour, such that the former is temperature sensitive but the latter is not.

We review model calculations based on a double Yukawa potential that exhibits some of the rich phase behaviour found experimentally, and predicting other behaviour which has not yet been found by experiment. Both the former and latter show a degree of similarity to the phase behaviour of polymer solutions. We also present preliminary results for the phase behaviour of bidisperse model sterically stabilized colloids.

1. Introduction

In a good solvent environment, with appropriate refractive index matching for stabilizing attached polymer species, monodisperse sterically stabilized colloidal dispersions may be regarded as archetypal hard-sphere systems. This finding allowed for some fine and impressive fundamental research on the behaviour of these model systems (see, for instance, [1]).

Actually the effective repulsive potential in sterically stabilized colloidal dispersions is softer than a hard-sphere repulsion. The colloidal stability of polystyrene lattices with adsorbed acidic polysaccharides has been found to increase with an increase in the steric layer thickness [2]. This, in turn, suggests that colloidal stability can be controlled by temperature, T, because T has important effects on the conformation of polymers and the solvent condition. Significant theoretical work on the conformation of polymers adsorbed at surfaces supports this conjecture. Earlier work is documented in the books by Napper [3] and de Gennes [4]; more recent work is referenced in the recent review by Szleifer [5]. We shall see below that, within the model we have put forward to account for the temperature dependence of the steric interaction, the temperature dependence acts in two ways: first on the steric layer thickness, second in uncovering deeper parts of the van der Waals attraction.

0953-8984/99/5010119+13$30.00

In developing our model effective potential we have taken into account the following experimental results.

(i) Non-aqueous dispersions of silica spheres stabilized by an adsorbed layer of C_{18} chains have been shown to display—on both heating and cooling—a reversible phase separation from a single homogeneous dispersed phase into a system of coexisting dilute and concentrated dispersed phases. This behaviour resembles the coexisting liquid and vapour phases of simple fluids. A similar behaviour has been also observed in depleted stabilized colloidal dispersions. Moreover, sterically stabilized colloidal dispersions show order–disorder transitions as a function of the dispersed phase concentration, similar to the melting/freezing transition in atomic and molecular systems [6, 7].

(ii) The phase diagram of sterically stabilized colloidal dispersions as a function of T and particle density ρ, or volume (packing) fraction η, is particularly remarkable due to the presence of both upper (high-T), and lower (low-T), two-phase coexistence regions. The experimental data of Edwards *et al* [8], following a procedure originally proposed and studied by van Helden *et al* [9], were obtained from silica spheres, each carrying a layer of terminally grafted C_{18}, dispersed in three different solvents with similar Hamaker constants. At higher temperatures the three *concave-up* coexistence curves are similar in shape but separated by temperature. This feature suggests that the thickness of the polymer coat does depend on the polymer–solvent interaction. At lower temperatures, three almost coincident *concave-down* curves appear in the composite phase diagram. At these lower temperatures the polymer coats are believed to be maximally stretched in all three systems and so should not influence the phase transition mechanism [10].

(iii) A colloidal system consisting of spherical silica particles, densely covered with linear hydrocarbon chains, is sterically stabilized when dispersed in a solvent such as toluene. An interesting aspect of the effect of temperature variation is a non-monotonic temperature dependence of the second virial coefficient $B_2(T)$ [11, 12].

In order to describe the preceding, and a few other, results we have proposed a double Yukawa potential, where we assume that the inverse decay length λ of the repulsive contribution is temperature dependent. In doing so we are assuming that the details of the polymer conformations are not as important as the thickness of the steric layer. We shall see below that, at least qualitatively, this assumption appears to reproduce the experimental trends referred to above.

We present, in the following sections, a brief review of work done using the above potential. We also present results for a bidisperse sterically stabilized colloidal dispersion. In section 2 we present the formalism used in our work: the double Yukawa potential and the Gibbs–Bogoliubov (GB) variational approach with which we carried out our calculations [13]. Results for the monodisperse case are reviewed in section 3.1, whereas results for the mixtures are presented in section 3.2. We sum up and briefly discuss our results in section 4.

2. Theory

The formalism presented below is written for the case of mixtures, of which the single-component system is a particular case.

The effective double Yukawa potentials (DY) we have proposed to account for the steric interactions read

$$v_{ij}(r) = \frac{E_{ij}\varepsilon_{ij}d_{ij}}{r}\left\{\exp\left[-\frac{A_{ij}}{d_{ij}}(\lambda_{ij}(T)r - d_{ij})\right] - \exp\left[-\frac{B_{ij}}{d_{ij}}(r - d_{ij})\right]\right\}. \tag{1}$$

The positive, dimensionless, coefficients E_{ij}, A_{ij} and B_{ij} are adjustable, and their parametrization is discussed in the next section. The λ_{ij} functions are assumed to depend only on temperature; d_{ij} and ε_{ij} are, respectively, the particle diameters and potential wells at $\lambda = 1$. The particle diameters are assumed to be additive, i.e. $d_{12} = \frac{1}{2}(d_1 + d_2)$, where d_i denotes the hard-sphere diameter of component i.

In the GB variational approach used in this work, the Helmholtz free energy F of a binary mixture with $N = N_1 + N_2$ particles, in a volume V, at temperature T satisfies the inequality

$$\frac{F}{Nk_BT} \equiv f \leqslant \tilde{f} = f^{HS} + f_1 \tag{2}$$

where f^{HS} denotes the reduced Helmholtz free energy of the hard-sphere (HS) reference system, and

$$f_1 = 2\pi\rho\beta \sum_{i,j} x_i x_j \int_0^\infty v_{ij}(r) g_{ij}^{HS}(r) r^2 \, dr. \tag{3}$$

In equation (3) ρ denotes the number density of the system, β is the inverse of T times the Boltzmann constant k_B, x_i the concentration of component i, such that $\sum x_i = 1$, and $g_{ij}^{HS}(r)$ the HS pair distribution functions.

The optimized free energy of the system is deduced by imposing the condition

$$\left(\frac{\partial \tilde{f}}{\partial \eta_i}\right)\Bigg|_{x_i,T} = 0 \tag{4}$$

where

$$\eta_i = \tfrac{1}{6}\pi\rho x_i d_i^3$$

is the HS packing fraction of component i. Then, for the values of η_i that satisfy equation (4), say η_i^{opt},

$$\tilde{f} \cong f$$

and the equation of state reads [14]

$$\frac{\beta P}{\rho} = 1 - \frac{2}{3}\pi\beta\rho \sum_{i,j} x_i x_j \int_0^\infty v'_{ij}(r) g_{ij}^{HS}(r) r^3 \, dr \tag{5}$$

where P denotes the pressure, and

$$v'_{ij}(r) = \frac{\partial v}{\partial r}.$$

The advantage of using this formalism with a DY potential is that both equation (3) and equation (5) can be written in a compact analytic form by using the analytic expressions of the Laplace transforms of the pair distribution functions in the Percus–Yevick (PY) approximation [15]. Following the work by Ashcroft and Foiles [16] (see also Gonzalez and Silbert [17]) for the one-component case, we use f^{HS} obtained from the PY virial equation of state [18]. Finally, we note that the chosen optimization procedure, equation (4), is not unique. We could have equally chosen the hard-sphere diameters, d_i, as the variational parameters, leading to the same variational equations for the Helmholtz free energy and the equation of state [14].

3. Results

We present below the results of our calculations. We consider first the effective monodisperse case, of which we review results, which have been either reported in the literature or in the PhD thesis of one of us (EC) [19]. The second part presents preliminary results of ongoing work for one particular case of a bidisperse system.

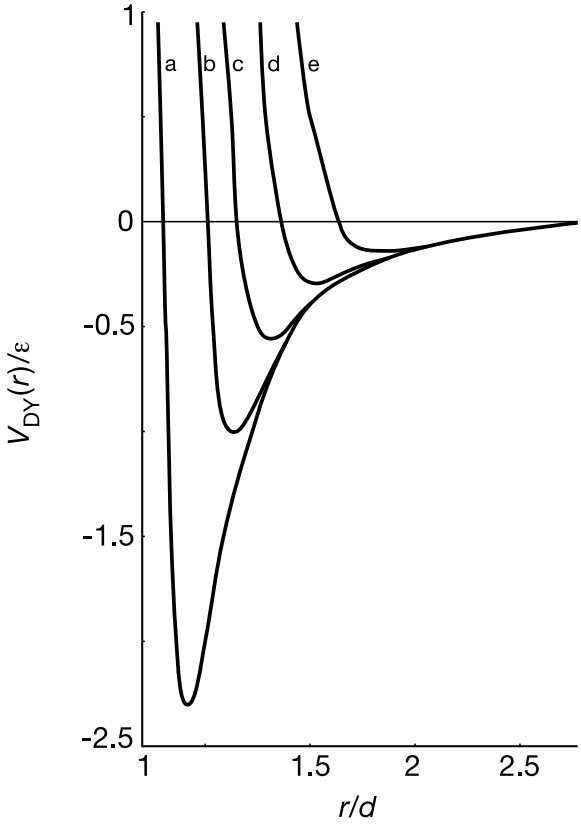

Figure 1. The effect of the collapse coefficient on the temperature dependent double Yukawa potential: (a) $\lambda = 1.2$; (b) $\lambda = 1.0$ (the 'Lennard-Jones' case; see text); (c) $\lambda = 0.9$; (d) $\lambda = 0.8$; (e) $\lambda = 0.7$ (after [22]).

3.1. Monodisperse system

The parameters A, B and E for the monodisperse case are fitted, for $\lambda = 1$, to mimic as closely as possible a 12–6 Lennard-Jones (LJ) potential. The choice of $A = 14.1867$, $B = 2.7369$ and $E = 2.0816$ is in accord with such requirement, and is similar to the values used in [16]. We have cross-checked our values for the parameters A, B and E by estimating the equilibrium cohesive energy, bulk modulus and elastic constants of a low-temperature LJ solid [20]. We have also calculated the liquid–solid transition using the Einstein model for the solid phase, and choosing Einstein's temperature

$$\theta_{\mathrm{E}} = \frac{\hbar\omega_{\mathrm{E}}}{k_{\mathrm{B}}T}$$

as the variational parameter (see Shih and Stroud [21]).

The introduction of $\lambda(T)$ into the repulsive term of the DY potential, equation (1), enables the potential to take on different shapes for different values of λ. This is illustrated in figure 1. We find that small variations in $\lambda(T)$—while preserving the form of the potential at large distances—results in a *soft-to-hard* transition in the form of the repulsive contributions to the potential, together with clear variations of the effective core diameter (namely the diameter of the dispersed particle plus the polymer coat). Although the attractive van der Waals interaction

between the macroparticles is only weakly dependent on T, mainly as a result of the temperature dependence of the Hamaker constant A_H, it is usual to assume that

$$\frac{A_H}{k_B T} \simeq 1$$

which we have used in our work. As for the repulsive part of the potential we note that, for values $\lambda \geqslant 1$, the depth of the potential becomes shallower. In this case our potential mimics a θ, or better than θ, behaviour for the polymer coat, very similar to the hard-sphere case. On the other hand, for values of $\lambda < 1$ the effective diameter becomes smaller, uncovering increasingly larger potential wells, and thus mimicking poor solvent conditions. Henceforth we call $\lambda(T)$ the *collapse coefficient*.

In order to calculate the phase behaviour of the system using the DY potential, we must specify the temperature dependence of the collapse coefficient. This choice is arbitrary. However, as we show below, the choices we make provide useful insights into the possible mechanisms of the phase behaviour of sterically stabilized colloids. We start by assuming a simple linear temperature dependence, namely

$$\lambda(T^*) = mT^* + n \tag{6}$$

where

$$T^* = \frac{k_B T}{\varepsilon}$$

denotes the reduced temperature. We have used two sets of values for m and n as shown in figure 2(a). The coefficients m and n in the line labelled A have the values

$$m_A^{-1} = 9.63 \qquad \text{and} \qquad n_A = 0.85$$

whereas in the line labelled B they have the values

$$m_B^{-1} = 0.602 \qquad \text{and} \qquad n_B = 0.7894.$$

We proceed to study the liquid–gas coexistence curves, for values of λ that lead to positive values of the pressure (for further details see [22]) by using the double-tangent construction. The results are shown in figure 2(b). It is possible to work out the coexistence curves for more complicated, but still linear, dependence of λ on T^* the details of which may be found in [22]. Within our model potential the existence of the upper coexistence curve is explained in terms of the collapse of the attached polymer layer with increasing temperature. We find that a linear increase in λ, caused by a linear increase in T, yields a not necessarily linear *soft-to-hard* transition with an associated small decrease of the core diameter, as indicated in figure 1. On the other hand, the lower coexistence curve arises from the van der Waals forces. At these lower temperatures the attached polymer chains are fully stretched and, likewise, the repulsive component of the DY potential is fully extended. The phase transition of this almost T-independent potential has the same mechanism as that of single-component Lennard-Jones systems.

We now turn to our results for the order–disorder transitions at high dispersed volume fractions; this is fully discussed by Canessa *et al* [23]. We assume λ to depend linearly on T^*, but with a smaller slope at low T^* and a larger slope at high T^*, as shown in figure 3(a). The phase behaviour which results from this $\lambda(T^*)$ is shown in figure 3(b). Here we find again the concave-down and concave-up coexistence curves shown in figure 2(b). Moreover we find *two* triple points where the colloidal solid, liquid and gas coexist. The freezing of the colloidal solid occurs when the packing fraction reaches the value $\eta \simeq 0.49$. In the results shown in figure 3(a), free energy considerations require the sterically stabilized colloidal solid to have an FCC structure. Note that the form of the phase diagram at high temperatures is sensitive to $\lambda(T^*)$.

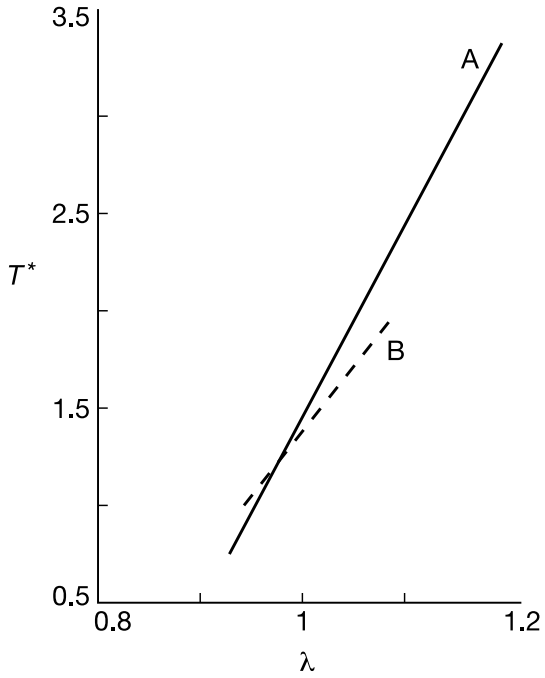

(a)

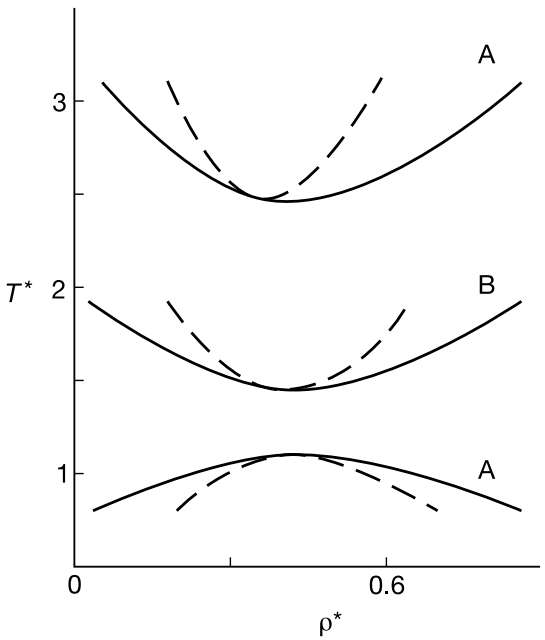

(b)

Figure 2. (a) Linear temperature variation of the collapse coefficient. The line A gives rise to the concave-up and concave-down phase separation curves labelled (A) shown in (b); the dotted line B gives rise to the intermediate concave-up coexistence curve (B), also shown in (b). (b) Calculated phase diagram of a sterically stabilized colloidal dispersion in the reduced temperature T^*–reduced density ρ^* plane which is obtained by using the $\lambda(T^*)$ shown in (a). Solid line: coexistence curves; dotted lines: spinodal curves.

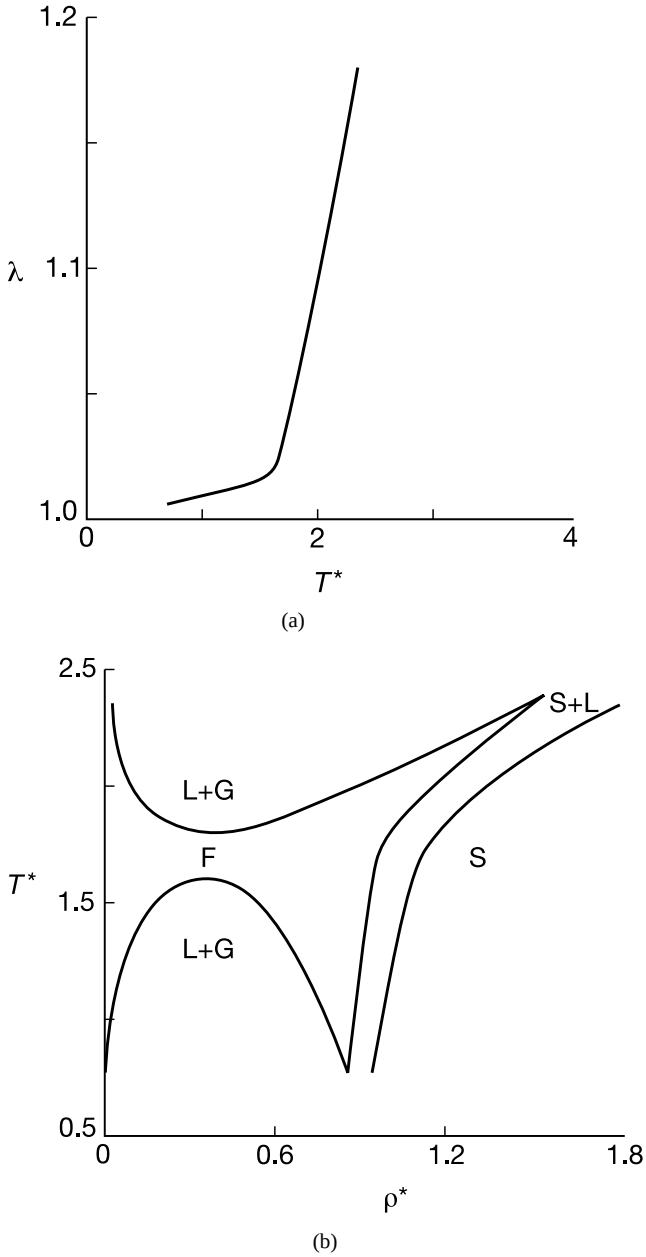

Figure 3. (a). Temperature dependence of the collapse coefficient used in the calculation of the phase diagram shown in (b). (b) T^*–ρ^* phase diagram of a sterically stabilized colloidal dispersion which is obtained by using the $\lambda(T^*)$ shown in (a). G, F, L and S denote the gas, fluid, liquid and solid phases respectively. L + G indicates the liquid–gas coexistence region, and similarly for S+L.

If we now assume that $\lambda(T^*)$ behaves as shown in figure 4(a), the (ρ^*–T^*) phase diagram of figure 4(b) is obtained [24], where $\rho^* = \rho d^3$ denotes the reduced density. If we consider the dotted-line form for $\lambda(T^*)$, an upper and lower liquid–vapour phase coexistence is obtained—enclosed by the dotted lines shown in figure 4(b)—where two regions of limited miscibility

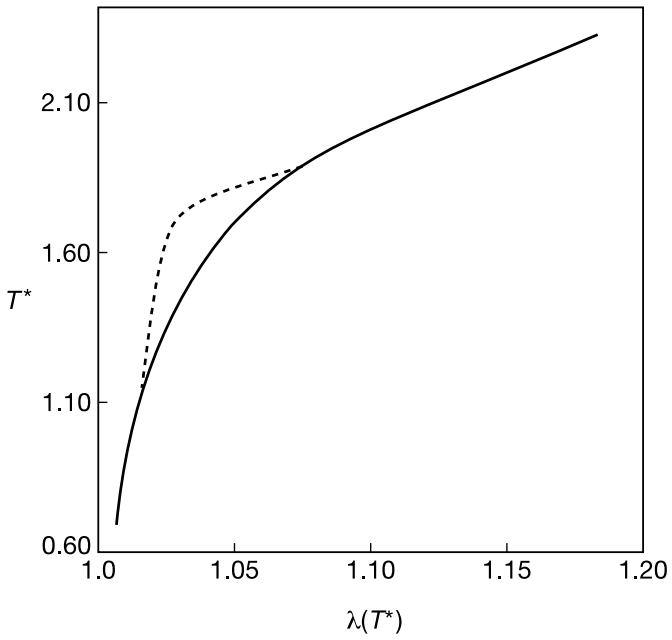

(a)

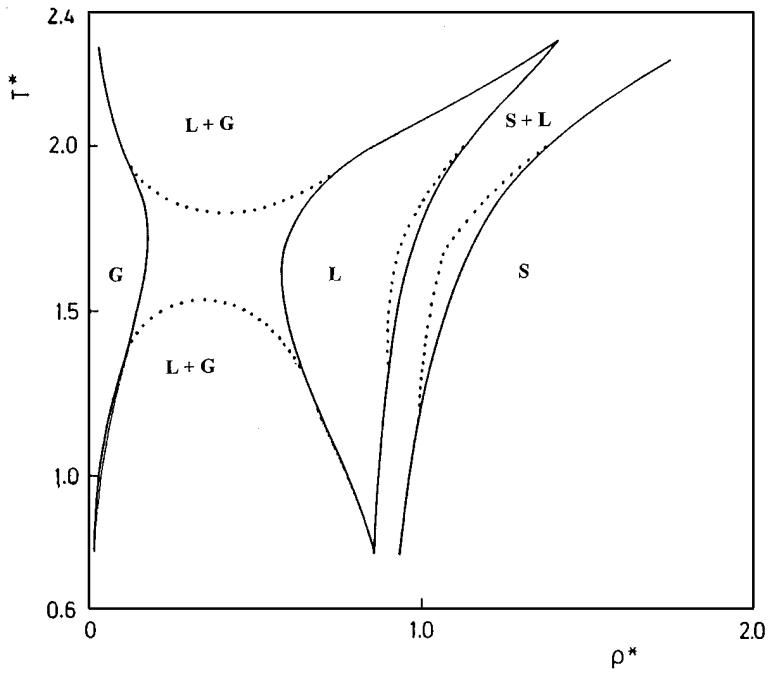

(b)

Figure 4. (a). Temperature dependence of the collapse coefficient. The dotted and solid lines give rise to the phase behaviour shown by dotted and solid lines in (b). (b) T^*–ρ^* phase diagram of a sterically stabilized colloidal dispersion which is obtained by using the $\lambda(T^*)$ shown in (a). G, L and S denote the gas, liquid and solid phases respectively. L + G indicate the liquid–gas coexistence region, and similarly for S + L. Note that only dotted lines enclose upper and lower liquid–vapour coexistence; the solid line exhibits an hourglass type phase transition (see text).

are present. These two phases are separated by a finite T interval. Moreover, one region lies below an upper critical temperature; the other lies above a lower critical temperature. As in the preceding case, the final form of the (ρ^*–T^*) phase diagram at high temperatures is very sensitive to the chosen $\lambda(T^*)$. If we now assume $\lambda(T^*)$ to have the form of the solid line in figure 4(a), the two phase separated regions now overlap, leaving only a very dilute and a more concentrated colloidal dispersion to exist independently as single phases. Such an unusual phase diagram has been observed in polymer solutions [25], where the two regions are known to overlap and to form an *hourglass* type of phase diagram, showing limited miscibility at all temperatures.

If the temperature dependence of $\lambda(T^*)$ shown in figure 3(a) is slightly altered such that λ once more attains a constant value at high T—which would physically occur if the polymer coating surrounding the macroparticle became compact—interesting changes appear in the phase diagram. The $\lambda(T^*)$ shown in figure 5(a) displays this class of behaviour which results in the phase diagram shown in figure 5(b). Compaction of the polymer layer is the key ingredient in producing the closed consolute line for the upper liquid–vapour two-phase coexistence region shown in figure 5(b). The closing of the upper two-phase regions arises because λ reaches an almost constant value after the system has already entered a two-phase region with increasing temperature. The closed consolute line is bounded above and below by critical points. Closed consolute lines are known to exist in miscellar systems [26], and in binary mixtures of organic liquids and water [27]. It would be very useful to investigate experimentally whether monodisperse sterically stabilized colloidal dispersions are actually capable of exhibiting the phase behaviour predicted in figure 5(b) by our model calculations. We note in passing that closed consolute lines have been predicted by van Roij *et al* [28] in their calculations of low-salt suspensions of charged stabilized colloidal particles.

3.2. Bidisperse systems

We present below preliminary results for a binary mixture of sterically stabilized colloids. We have chosen the following parametrization. We assume that the parameters E_{ij}, A_{ij} and B_{ij} have each the same values E, A and B respectively, and these are given by those chosen for the monodisperse case. We have further assumed that $\lambda(T^*)$ is the same for both components, and is given by the linear behaviour labelled A in figure 2(a). For the other coefficients we are taking values which are in reasonable agreement with those corresponding to the Ar–Kr binary mixture [29]. However, unlike the monodisperse case, we have yet to check out whether our results for $\lambda = 1$ reproduce the Monte Carlo results shown in [29]. These values are:

$$\alpha = \frac{d_1}{d_2} = 0.8 \qquad \kappa = \frac{\varepsilon_{11}}{\varepsilon_{22}} = 0.72 \qquad \text{and} \qquad \zeta = \frac{\varepsilon_{12}}{\sqrt{\varepsilon_{11}\varepsilon_{22}}} = 0.98.$$

In order to carry out calculations of the phase behaviour as a function of concentration it is necessary to evaluate the derivative of the Gibbs free energy G, at a given T, at all concentrations for different values of the pressure P. Then, at a given pressure, we obtain the values of the concentrations x_{G} and x_{L} of the mixture for gas (G) and liquid (L) phases in equilibria. These calculations are repeated for different values of P. Even within our model the calculations, while reasonably straightforward, are lengthy. Moreover, some care needs to be taken in the calculations of excess properties. Recall that $G/Nk_{\mathrm{B}}T$ is obtained directly from equations (2) and (5), using standard thermodynamic relations. Figure 6 shows the pressure–concentration 'gas–liquid' equilibria at the end rich in component 2 (in figure 6, $x = x_1 = 1-x_2$ at $T^* = 0.8$). We find that both gas and liquid phases converge towards what appear to be a critical point. More calculations are in progress and will be reported on completion.

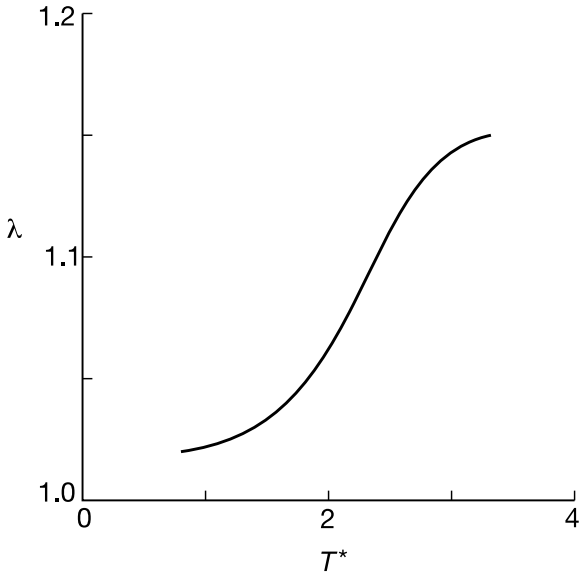

(a)

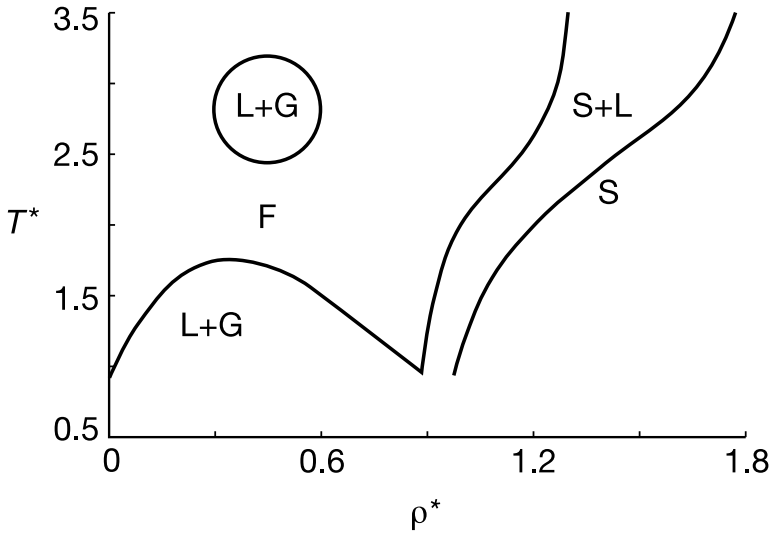

(b)

Figure 5. (a) Temperature dependence of the collapse coefficient used in the calculation of the phase diagram shown in (b). (b) T^*–ρ^* phase diagram of a sterically stabilized colloidal dispersion which is obtained by using the $\lambda(T^*)$ shown in (a). G, F, L and S denote the gas, fluid, liquid and solid phases respectively. L + G indicates the liquid–gas coexistence region, and similarly for S + L.

4. Discussion

In the preceding section we presented results for the phase behaviour of monodisperse and bidisperse sterically stabilized colloidal dispersions based on the assumptions of a very simple model effective pairwise additive, temperature dependent, double Yukawa potential which qualitatively predicts reasonable phase diagrams for these systems.

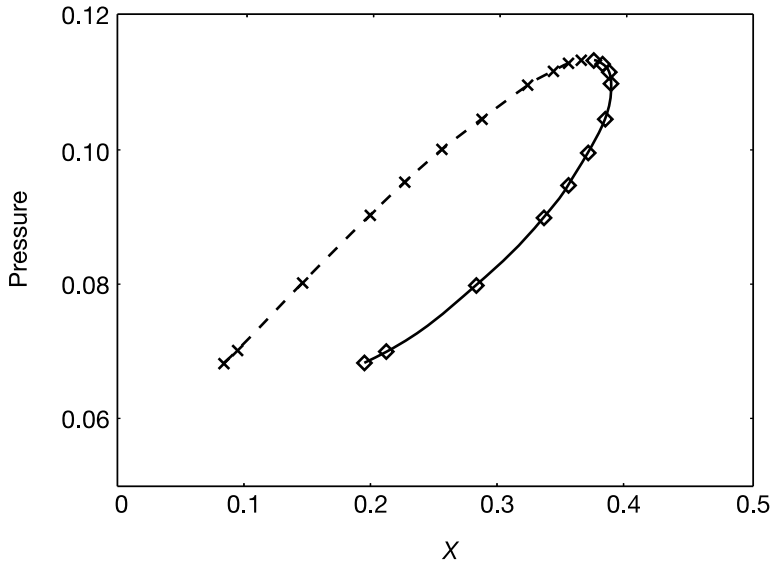

Figure 6. Pressure–concentration gas–liquid equilibria at the rich end of component 2 of a bidisperse sterically stabilized colloidal dispersion at $T^* = 0.8$, using the collapse coefficient shown as (A) in figure 2(a). The pressure is given in reduced units and the concentration $x = x_1 = 1 - x_2$. Squares denote the gas phase, crosses the liquid phase; broken and solid lines are guides to the eye, in order to show the region of gas–liquid equilibrium. Note that the squares and crosses appear to converge to a critical point (not shown).

The key to our model potential is the assumption that the inverse decay length of the repulsive Yukawa, the collapse coefficient, depends on temperature. Since the core of the double Yukawa potential is viewed as comprising the dispersed solid particles and their polymer coating, variations of the polymer layer thickness with temperature characterize $\lambda(T^*)$. This assumption is supported by established, semi-empirical, theories of polymer solutions. Canessa *et al* [23] used the Flory–Huggins (FH) theory [30] to relate a chain collapse to a decrease in solvent quality with temperature, assuming that the exchange energy in the FH theory varies linearly with T. Moreover, Gallego *et al* [31] examined the relationship between the one-component macroparticle approach, discussed in the preceding section, and the Scheutjens–Fleer (SF) [32] model for the interaction of planar surfaces with adsorbed polymer layers. SF introduced a mean field theory for a lattice model of polymer adsorption that constitutes a generalization of the FH theory to the case of inhomogeneous systems. In restricted equilibrium, namely when the total amount of adsorbed polymer between the plates is constant, Gallego *et al* have shown that the SF model exhibits a decrease in the polymer layer thickness with increasing T, consistent with our one-component macroparticle model. We are assuming that similar results will prevail in the binary mixture case.

There appear to be similarities between the phase behaviour predicted by our model for sterically stabilized colloidal dispersions and that found experimentally for polymer solutions. Experimentally only one case has been found where these similarities do exist. Our results suggest that there is a case to explore experimentally such similarities even further.

The results obtained with our DY model potential provide two important insights that any fundamental theory must take into account. First, they suggest that the details of the polymer conformations are not too important; only the amount of stretching and compaction appear to matter. Note that the polymer functionality is only grossly taken into account by the different

temperature dependence assumed for the collapse coefficient. Second, they also suggest that it is not possible to separate out the free energy contributions due to the polymer conformations from the polymer–solvent interaction, namely the solvent quality as a function of T. To our knowledge Doland and Edwards [33] were the first to attempt to overcome this difficulty.

On attempting to develop a robust theory for the effective interactions in sterically stabilized colloidal dispersions, it is no longer possible to proceed as in the cases of either charge [34] or depletion [35] stabilized colloidal dispersions. In both these cases, within some constraints, the effective Hamiltonian of the macroparticles can be written, in the canonical ensemble formalism, as

$$H_{\mathrm{eff}} = H_{\mathrm{m}} + F' \tag{7}$$

where H_{m} is the direct, or bare, Hamiltonian of the macroparticles, and F' is the Helmholtz free energy of the 'other particles' in the external field of a fixed configuration of the macroparticles (in charge stabilized colloidal dispersions, the 'other particles' include the counterions, coions and added salt particles; in depletion stabilized colloids, the 'other particles' are the free polymers). In equation (7) F' is a function of the instantaneous positions of the macroparticles and the thermodynamic state of the system. However, the partition function of the 'other particles', integrates out their degrees of freedom, namely their positions and momenta. This procedure cannot be carried out in sterically stabilized colloids because the polymers are attached to the macroparticles. Hence the partition function depends not only on the positions and momenta of the polymers but also on the relative positions of the macroparticles. Here a new approach is needed. Promising progress has been reported by Löwen and coworkers [36], but much more remains to be done before the theory for the effective interactions in sterically stabilized colloidal dispersions is regarded as being in a satisfactory state.

Acknowledgments

We are very grateful to Gary Barker, David Gonzalez and Peter Richmond for many useful discussions over the years on several aspects of this work. OHS and MS thank Guillermo Zarragoicoechea for his help with some of the numerical aspects of the binary mixture calculations. The same two authors gratefully acknowledge the financial support of Fundación Antorchas and The British Council.

References

[1] Pusey P N 1991 *Liquids, Freezing and Glass Transition* ed J-P Hansen, D Levesque and J Zinn-Justin (Amsterdam: Elsevier) p 763
[2] Yokoyama A, Srinivasan K R and Fogler H S 1990 *Langmuir* **6** 702
[3] Napper D H 1983 *Polymeric Stabilization of Colloidal Dispersions* (London: Academic)
[4] de Gennes P-G 1979 *Scaling Concepts in Polymer Physics* (Ithaca, NY: Cornell University Press)
[5] Szleifer I 1996 *Curr. Opinion Colloid Interface Sci.* **1** 416
[6] Vincent B 1987 *Colloids Surf.* **24** 269
[7] Vincent B, Edwards J, Emmett S and Groot R 1988 *Colloids Surf.* **31** 267
[8] Edwards J, Everett D H, O'Sullivan T, Pangalou I and Vincent B 1984 *J. Chem. Soc. Faraday Trans.* I **80** 2599
[9] van Helden A K, Jansen J W and Vrij A 1981 *J. Colloid. Interface Sci.* **79** 289
[10] Eshuis A, Harbers G, Doornink D J and Mijnkieff P F 1985 *Langmuir* **1** 289
[11] Jansen J W, de Kruif C G and Vrij A 1986 *J. Colloid. Interface Sci.* **114** 492
[12] Canessa E, Grimson M J and Silbert M 1988 *Phys. Chem. Liq.* **18** 287
[13] Isihara A 1968 *J. Phys. A: Math. Gen.* **1** 539
[14] Watabe M and Young W H 1974 *J. Phys. F: Met. Phys.* **4** L29
[15] Lebowitz J L 1964 *Phys. Rev.* A **133** 895
[16] Foiles S M and Ashcroft N W 1981 *J. Chem. Phys.* **75** 3594

[17] Gonzalez D J and Silbert M 1983 *J. Phys. C: Solid State Phys.* **16** L1097
[18] Lebowitz J L and Rowlinson J S 1964 *J. Chem. Phys.* **41** 133
[19] Canessa E 1989 *PhD Thesis* University of East Anglia
[20] Canessa E, Grimson M J and Silbert M 1987 *Solid State Commun.* **64** 145
[21] Shih W H and Stroud D 1983 *J. Chem. Phys.* **79** 6254
[22] Canessa E, Gonzalez D J, Grimson M J and Silbert M 1988 *Mol. Phys.* **64** 207
[23] Canessa E, Grimson M J and Silbert M 1989 *Mol. Phys.* **67** 1153
[24] Canessa E and Grimson M J 1989 *Colloid. Polym. Sci.* **268** 972
[25] Marra J and Hair M L 1988 *Macromolecules* **21** 2356
[26] Meroni A, Pimpinelli A and Reatto L 1987 *Chem. Phys. Lett.* **135** 137
[27] Tamaki S 1989 *Phase Transitions* **66** 167
[28] van Roij R, Dijkstra M and Hansen J-P 1999 *J. Phys.: Condens. Matter* **50** 10 047–60
[29] McDonald I R 1973 *Statistical Mechanics: Specialist Periodical Reports* vol 1, ed K Singer (London: Chemical Society) p 134
[30] Flory P J 1953 *Principles of Polymer Chemistry* (Ithaca, NY: Cornell University Press)
[31] Gallego L J, Grimson M J, Rey C and Silbert M 1992 *Colloid. Chem. Phys.* **270** 1091
[32] Scheutjens J M H M and Fleer G J 1985 *Macromolecules* **18** 1882
[33] Doland A K and Edwards S F 1975 *Proc. R. Soc.* A **343** 427
[34] Grimson M J and Silbert M 1991 *Mol. Phys.* **74** 397
van Roij R, Dijkstra M and Hansen J-P 1999 *Phys. Rev.* E **59** 2010
Denton A R 1999 *J. Phys.: Condens. Matter* **50** 10 061–71
[35] Barker G C, Grimson M J and Silbert M 1995 *Mol. Phys.* **84** 211
Dijkstra M, van Roij R and Evans R 1999 *Phys. Rev.* E **59** 5744
[36] Likos C N, Löwen H, Watzlawek M, Watzlawek M, Abbas B, Jucknischke O, Allgaier J and Richter D 1998 *Phys. Rev. Lett.* **80** 4450
Watzlawek M, Likos C N and Löwen H 1999 *Phys. Rev. Lett.* **82** 5289
Watzlawek M, Likos C N and Löwen H 1999 *J. Phys.: Condens. Matter* at press